THE QUADRUPOLAR COMPONENT OF THE ESS LINAC PROTON BEAM

B. Bolling*, N. Milas, European Spallation Source, Lund, Sweden
J. Cederkäll, B. Meirose, Department of Physics, Lund University, Lund, Sweden

Abstract

Beam Position and Phase Monitors (BPMs) are used as part of normal routines to measure the dipole component of a charged particle beam in order to determine its transverse position. However, BPMs are also sensitive to higher-order moments of the beam charge distribution, including the quadrupolar component, which provides access to the difference in horizontal and vertical beam RMS sizes. This work investigates the feasibility of extracting the quadrupolar component of the proton beam of the ESS superconducting linac (SCL) through the BPMs. The theoretical framework for quadrupolar signal formation is reviewed, with emphasis on the relation between pickup sensitivities and beam parameters, and a calibration strategy based on measuring the quadrupolar signal sensitivity with respect to the beam centroid position.

INTRODUCTION

BPMs constitute a fundamental diagnostic tool in particle accelerators, providing information on the dipole component of the beam to determine its horizontal and vertical positions, including at ESS [1]. Beyond position, BPMs are sensitive to higher-order moments of the beam charge distribution, including the quadrupolar component, which encodes information about the difference in horizontal and vertical beam sizes. Access to this information enables non-invasive monitoring of beam shape asymmetries and contributes to improved optics matching and beam quality control.

The ESS superconducting linac (SCL) provides a unique opportunity to exploit quadrupolar BPM signals for high-power proton beams. This paper develops the theoretical basis for quadrupolar signal formation, proposes a methodology for calibration and validation, and outlines a measurement strategy at ESS using BPMs. Figure 1 illustrates the design of the BPMs in the Spoke (SPK) section of the ESS SCL and the rest of the ESS SCL (MBL, HBL and HEBT sections, also referred to as elliptical sections) with the following differences between BPM aperture diameters:

- SPK section BPMs: d = 57.1 mm
- Elliptical sections BPMs: d = 100 mm

The BPMs in the ESS SCL are located in so-called Linac Warm-Units (LWUs), each typically including a focusing (QH) and defocusing (QV) quadrupole magnet pair, and a BPM and a combined corrector magnet in-between the quadrupole doublet.

The quadrupolar component is defined as

$$\Xi = \sigma_x^2 - \sigma_y^2 + \bar{x}^2 - \bar{y}^2, \tag{1}$$

* benjamin.bolling@ess.eu

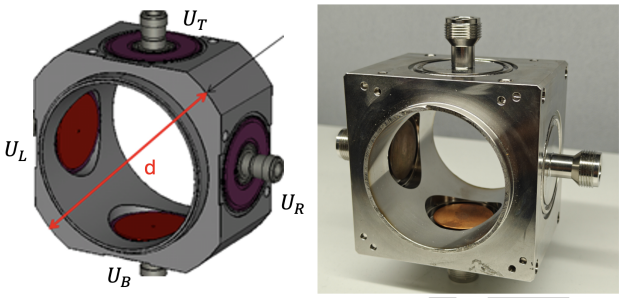

Figure 1: SPK and elliptical (MBL, HBL, HEBT) LWU sections' BPM design (left) and a SPK BPM photograph (right).

where σ_x and σ_y are the rms beam sizes in the two transverse planes, and $(\bar{x}, \bar{y})$ are the beam centroid position offsets relative to the BPM electrical center.

Following the formalism of [2,3], the voltages, U, induced in the four BPM electrodes (R, L, T, B) contain both dipole and quadrupolar terms which in normalized form yields the quadrupolar BPM signal by

$$\Xi_{\Delta/\Sigma} = \frac{U_L + U_R - U_T - U_B}{U_L + U_R + U_T + U_B} = S_Q \left(\sigma_x^2 - \sigma_y^2 + \bar{x}^2 - \bar{y}^2\right) \tag{2}$$

where S_Q is the quadrupolar sensitivity, dependent on the BPM aperture and electrode geometry. Beam centroid positions are obtained from the dipole terms:

$$\Delta_x = \frac{U_L - U_R}{U_L + U_R}, \qquad \Delta_y = \frac{U_T - U_B}{U_T + U_B}. \tag{3}$$

Due to the unavailability during the time of study of beam invasive diagnostic instruments to directly measure the beam profile at given locations, the sensitivities S_Q were calculated based on BPM design parameters and through calibration.

CALIBRATION AND DATA ANALYSIS

The characterization of the quadrupolar response across the ESS SCL was performed by scanning the beam centroid using corrector magnets upstreams the BPMs used for measurements. To extract the sensitivity S_Q, the experimental data were fitted to eq. (2) which can be directly identified from the curvature coefficient $a \equiv S_Q$. This calibration is inherently independent of the beam intensity, relying solely on the transverse distribution of charged particles in the beam.

Operational constraints during the beam studies occasionally resulted in scans performed with a non-zero offset in the non-scanning plane (e.g., a vertical offset $\bar{y}_0$ during a horizontal scan). This offset introduces a parasitic shift in the signal baseline. To recover the real geometric response, a correction protocol was implemented to "align" the data

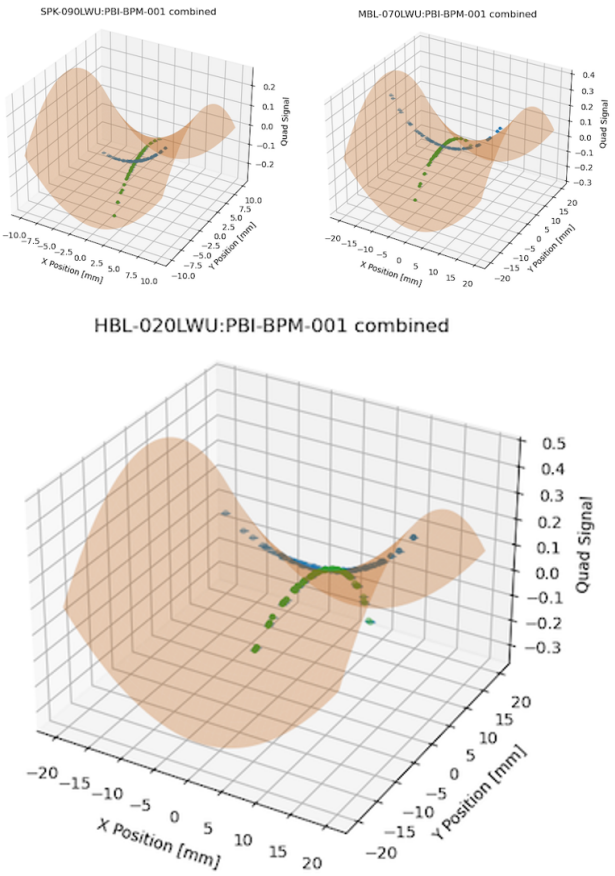

Figure 2: Calibration surfaces for selected BPMs

points utilizing a fitting as a function of both the horizontal and vertical offset, i.e.,

$$\Xi_{\Delta/\Sigma} = S_Q\left(\bar{x}^2 - \bar{y}^2\right) + c \tag{4}$$

where $c = S_Q(\sigma_x^2 - \sigma_y^2)$ is considered to be constant.

To visualize the fitting, two-dimensional surface fits of the quadrupole signal were employed considering the offset originating from σ_x^2 and σ_y^2 in accordance with eq. (2). The resulting calibration surface functions are plotted in Fig. 2 for three selected BPMs from the SPK, MBL and HBL sections.

Table 1 summarizes the extracted coefficients for all BPMs in the sections SPK, MBL and HBL. It also includes the column S_t denoting the theoretical displacement sensitivity of each BPM, which is linked to the linear position response ($\Delta_x \approx x/S_x$ and $\Delta_y \approx y/S_y$).

A clear step-change in S_Q is observed between the Spoke (SPK) and Medium-Beta (MBL) sections, accurately reflecting the mechanical increase in beam pipe radius. Furthermore, the symmetry between horizontal and vertical extractions validates the geometric integrity of the BPM pick-up electrodes. Analysis of the fit coefficients reveals high consistency across the linac sections.

The ratio between the measured results' extracted sensitivities S_Q of the SPK and elliptical sections' BPMs is 3.3 whilst the corresponding ratio for the theoretical $S_t^2 \approx 3.27$, which indicates excellent agreement (within 1%) confirming

Table 1: Comparison of extracted fit coefficients of the quadrupolar component of the beam averaged for each section and over the horizontal and vertical scans.

	$S_{Q,\mathrm{calc}}$ $10^{-4}[\mathrm{mm}^{-2}]$	$S_{Q,\mathrm{meas}}$ $10^{-4}[\mathrm{mm}^{-2}]$	c_{meas} 10^{-2}
SPK	101.2	26.0 +/- 0.5	4.98 +/- 0.2
MBL	30.8	7.87 +/- 0.3	3.61 +/- 0.2
HBL	30.8	8.14 +/- 0.3	0.929 +/- 0.3

that the calibration is able to capture the mechanical scaling of the BPMs in the physical machine. This provides high confidence in the transfer of the calibration values to the analysis of the quadrupolar component of the beam utilizing the BPMs in the HEBT section of the machine.

BEAM QUADRUPOLAR COMPONENT MEASUREMENTS

To verify the longitudinal mapping of the lattice, independent perturbations of the beam were performed using quadrupole pairs at different locations (HEBT-010 and HEBT-080). Measurements were done at two separate occasions, once with a 90 MeV beam and once with a 800 MeV beam. The 90 MeV study was performed as a proof of principle, resulting in that the BPM sensitivity was sufficient to measure the quadrupolar component of the beam and with no energy dependency given that the same results were obtained with both the 90 MeV and the 800 MeV beam.

As the BPMs in the MBL, HBL and HEBT sections have identical mechanical geometry, MBL calibration results as defined in Table 1 were transferred and implemented as part of the analysis of the measurement results in order to derive the beam quadrupolar component from the measured BPM quadrupolar signal. Figure 3 illustrates the oscillations induced by these perturbations through HEBT-080LWU quadrupole magnets scans and measured through the BPMs in the figures to the left, with the data for this plot acquired during the 800 MeV beam.

The HEBT-080 scan reveals that the quadrupolar response remains unchanged for the first eight BPMs, with a discrete divergence appearing only from HEBT-090. This response confirms the localized nature of the beam envelope modulation, with high-amplitude oscillations observed downstream of the perturbation source providing a benchmark for the lattice phase advance and hence allows for detection of gradient scaling errors in individual magnets' magnetic fields.

MODEL COMPARISON

To evaluate the accuracy of extracted beam quadrupolar component, the experimental results were qualitatively compared against numerical simulations with Open XAL [4] and the ESS lattice configuration. With the plots on the left in Fig. 3 illustrating the measured beam quadrupolar component and its differential response for quadrupole perturbations, the corresponding simulated behaviour can be compared to through the right plots in Fig. 3. The numerical

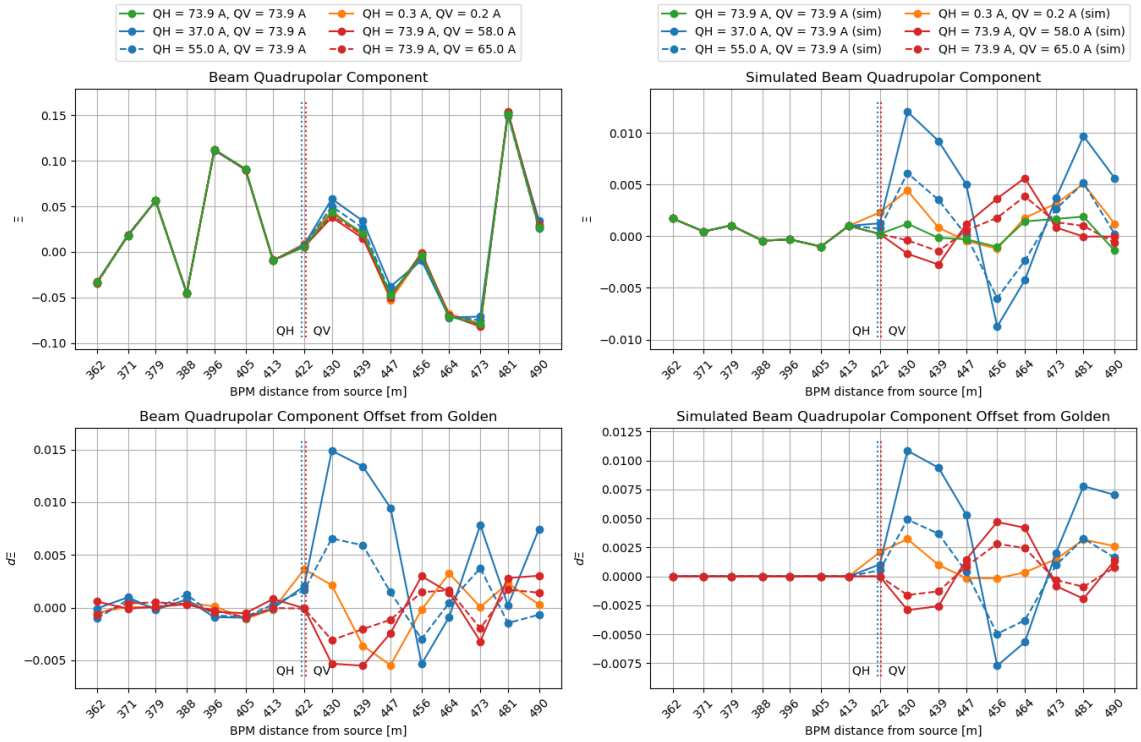

Figure 3: Perturbation of a QH and QV pair situated in the HEBT-080 LWU (with the blue and red dotted lines annotating their respective location) and the resulting BPM responses. The top plots shows the beam quadrupolar component for the ”Golden” setting (green line) and perturbations in the other lines, whilst the bottom plots shows the offsets from the ”Golden” setting of these perturbations. The left plots show measured results and the right plots show simulated results.

simulations have been performed using the ESS lattice configuration of the HEBT section to serve as the benchmark for the experimental data, including FODO focusing structures and accelerating modules.

The top plots of Fig. 3 show the calibrated beam quadrupolar component where raw quadrupolar signals from the BPMs have been processed using S_Q from Table 1. A comparison reveals that there is a discrepancy between the model and the measurement prior and following the location of the perturbation attributed to initial beam mismatch, including unknown Twiss parameters at the HEBT section entrance.

Analysis of the bottom plots of Fig. 3, i.e., the ”Offset from Golden”, the parasitic effects of the mismatched beam envelope becomes suppressed. This allows for a direct comparison of how the beam envelope responds to the perturbations. The measurement and simulation show a qualitative agreement in the oscillations downstream of the HEBT-080LWU (the perturbation source location). This suggests that the lattice phase advance in the model can be considered as representative of the physical machine.

CONCLUSIONS AND OUTLOOK

This work demonstrated the feasibility of extracting the beam quadrupolar component using the standard BPM system at the ESS SCL. The implementation of a 2D surface-fitting calibration decoupled geometric sensitivities from parasitic beam drifts, establishing calibration factors that scale accurately with the mechanical aperture of the BPM species included in the study.

While the ”Offset from Golden” measurements (Fig. 3) show a qualitative agreement in phase with the OpenXAL model (apart from minor qualitative discrepancies observed in the phase alignment and amplitude evolution), significant quantitative discrepancies of the oscillations following the perturbation remain. The measured absolute quadrupolar component is approximately an order of magnitude larger than the design model, and the simulation shows a higher sensitivity to magnetic field changes than observed in the physical machine. These differences suggest that the study is currently limited by uncertainties in the initial beam distribution and potential systematic offsets in the absolute normalization of the quadrupolar signal.

Future work includes improving the qualitative analysis followed by

- **Further tests:** Required in order to understand the discrepancies between the simulated and measured results.
- **Initial State Reconstruction:** Employing Machine Learning, Emittance Measurement Units, and/or inverse-matching algorithms to determine the incoming Twiss parameters.
- **Firmware Integration:** Developing automated, real-time extraction routines within the FPGA-based BPM electronics for continuous beam shape monitoring.

ACKNOWLEDGMENTS

The authors would like to thank R. Baron (ESS Beam Diagnostics Group) for providing the technical design specifications and mechanical sensitivity constants for the various BPM species at ESS, as well as the diagnostic hardware illustrations. We especially appreciate their continuous availability for technical discussions and expert support.

REFERENCES

[1] R. Baron *et al.*, "ESS beam position and phase monitor System", in *Proc. IBIC'19*, Malmö, Sweden, pp. 543–547, Sep. 2019. doi:10.18429/jacow-ibic2019-wepp015

[2] J. A. T. Kamga, W. F. O. Müller, and T. Weiland, "Analytical and numerical calculation of the second-order moment of the beam using a capacitive pickup", *Phys. Rev. Accel. Beams*, vol. 19, no. 4, Apr. 2016. doi:10.1103/physrevaccelbeams.19.042801

[3] D. Alves, M. G, and T. Lefèvre, "Analysis of Quadrupolar Measurements for Beam Size Determination in the LHC", in *Proc. IBIC'19*, Malmö, Sweden, Sep. 2019, pp. 397–401, 2019. doi:10.18429/JACoW-IBIC2019-TUPP034

[4] OpenXAL Collaboration, "Openxal: an open source accelerator physics software platform", https://openxal.github.io,